ACS APPLIED MATERIALS & INTERFACES

Research Article

www.acsami.org

Femtosecond Laser Treatment for the Design of Electro-insulating Superhydrophobic Coatings with Enhanced Wear Resistance on Glass

Ludmila B. Boinovich,*[,†] Alexandre G. Domantovskiy,[‡] Alexandre M. Emelyanenko,[†] Andrei S. Pashinin,[†] Andrey A. Ionin,[§] Sergey I. Kudryashov,[§] and Pavel N. Saltuganov[§,∥]

[†]A. N. Frumkin Institute of Physical Chemistry and Electrochemistry, Leninsky prospect 31 bld. 4, 119071 Moscow, Russia

[‡]National Research Centre "Kurchatov Institute", Akademika Kurchatova sq., 1, 123182 Moscow, Russia

[§]P. N. Lebedev Physical Institute, Russian Academy of Sciences, Leninsky prospect 53, 119991 Moscow, Russia

[∥]Moscow Institute of Physics and Technology (National Research University) "MFTI", Moscow, Russia

ABSTRACT: Femtosecond laser treatment of a glass surface was used to fabricate a multimodal roughness having regular surface ripples with a period of a few micrometers decorated by aggregates of nearly spherical nanoparticles. UV−ozone treatment followed by chemisorption of the appropriate functional fluorosilanes onto the textured surface makes it possible to fabricate a superhydrophobic coating with a specific surface resistance on the order of petaohms on a glass surface. The main advantage of the fabricated coating under severe operating conditions with abrasion loads is the significant durability of its electro-insulating properties. The longevity of the high surface resistivity, even on long-term contact with a water vapor-saturated atmosphere, is directly related to the peculiarities of the surface texture and ripple structure.

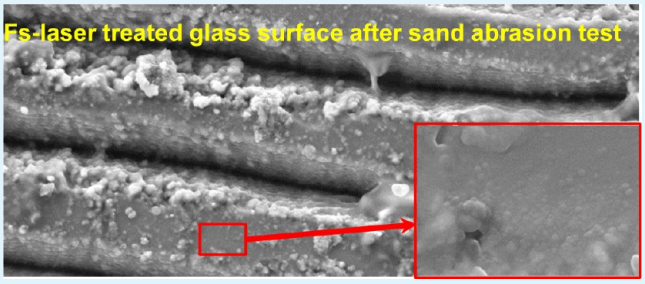

KEYWORDS: *superhydrophobicity, wetting, surface electric resistance, femtosecond laser treatment, abrasive resistance, electro-insulating coatings*

INTRODUCTION

Over the past few decades, glasses have played an increasingly important role as construction, optical, and electrotechnical materials. For example, glass materials are widely used as electro-insulating materials in electroenergetics for outdoor use. However, in many cases, the surface treatment of these materials is required to enhance the functionality of glass-based construction elements. Leakage currents along both glass insulator surfaces and the insulating surface of dischargers for atmospheric overvoltage protection are one of the main problems in overhead power lines and electrical substations, as well as electrified railways and municipal transport lines. These currents are especially high when glass insulators well wetted by water are moistened by precipitation. Superhydrophobicity has been proposed as a promising strategy for the surface treatment of materials intended for outdoor engineering applications.[1−9] The most attractive features of superhydrophobic coatings for electroenergetic applications include, among others, water repellency, low adhesion of liquid drops to such a surface resulting in the removal of the drop from the surface under wind or vibration load, self-cleaning properties, and the absence of thick water wetting layers on this surface under saturated vapor conditions.[10] In addition, the surface electrical conductivity of superhydrophobic coatings fabricated using nonconductive hydrophobic agents is very low because of the excellent electro-insulating properties of the latter. A wide variety of methods for fabricating superhydrophobic coatings on glass surfaces have recently been developed.[1,5−9,11−16]

The strategy for designing these coatings involves finding solutions to three problems:[17] decreasing the surface energy of a material, increasing the local Young contact angle of a textured surface by choosing the appropriate shape of textural elements, and the formation of a texture with multimodal roughness on the surface. The first problem is easily solved today by treating the surface with hydrophobic agents. As described in recent reviews,[18,19] femtosecond laser surface texturing has emerged as a novel and versatile technology for producing surfaces with multimodal roughness and high curvature of textural elements suitable for a wide range of applications. In this paper, we will show that femtosecond laser surface structuring followed by UV−ozone treatment and hydrophobization of the textured surface by the appropriate functional fluorosilanes make it possible to fabricate electro-insulating superhydrophobic coatings on glass insulators for

Received: November 16, 2013
Accepted: January 23, 2014
Published: January 23, 2014

overhead power lines operating under severe environmental conditions.

MATERIALS AND METHODS

In this work, we fabricated and studied superhydrophobic coatings on the surface of glass slides with the following chemical composition: 70 wt % SiO_2, 11 wt % Na_2O, 7 wt % CaO, 4.5 wt % K_2O, 4.2 wt % ZnO, 1.5 wt % BaO, and 1.8 wt % other oxides (Matsunami Glass Ind., Ltd.). Hydrophobic coatings were prepared on substrates from the same glass for comparison. The hydrophobic agent methoxy-{3-[(2,2,3,3,4,4,5,5,6,6,7,7,8,8,8-pentadecafluorooctyl)oxy]propyl}silane, synthesized in the laboratory, was used to prepare both the hydrophobic and superhydrophobic coatings on a smooth or textured glass surface. For this purpose, the samples were immersed in a 2% solution of hydrophobic agent in 99% decane (Acros Organics) for 2 h and then dried in an oven at 120 °C for 60 min.

We used femtosecond laser treatment for surface texturing to meet the criteria necessary for obtaining superhydrophobicity. This method employs different relief generation principles on nano- and micro-scales. Regular surface ripples with periods of a few micrometers (in some cases, with periods of <100 nm[20]) are fabricated by surface interference of the incident femtosecond laser pulses and their surface-scattered replica[21] existing in the form of surface electromagnetic waves (surface plasmon polaritons) with wavelengths slightly shorter than the laser wavelength.[22] The resulting removal of the ablative material from the interference maxima yields surface ripples. Likewise, femtosecond laser surface microstructuring in the form of quasi-regular microspikes also relies on laser diffraction on separate surface sub- and microroughness features (spikes and ridges), resulting in spatially inhomogeneous absorption and ablation.[23] However, the subsequent evolution of separate ridges occurs via their multiplication and self-organization because of the positive (weaker absorption and ablation and stronger redeposition of nanoparticles) and negative (stronger absorption and ablation) optical feedbacks for ridges and valleys, respectively. As a result, both of these multimodal surface relief structures appear and develop spontaneously during multishot femtosecond laser exposures, allowing large-scale surface structuring.

In this work, a Satsuma Yb-doped fiber laser (Amplitude Systèmes) delivered 200 fs (full width at half-maximum), frequency-doubled (second-harmonic wavelength of 515 nm) pulses with a maximal energy of 4 μJ in TEM_{00} mode. The pulses were coming at repetition rate f, which was varied by an off-resonator acousto-optic modulator at the laser output. The initial 1 mm beam diameter was expanded using a two-lens telescope to fill the 25 mm aperture of a silica glass lens (focusing distance of 35 mm), focusing it into a 7 μm wide (the $1/e^2$ level) focal spot with peak fluence F of $\approx$5 J/cm^2 onto a glass sample surface. The samples were raster scanned at linear speed v in a number of overlapping lines with overlap step l to produce a homogeneous surface texture with regularly spaced trenches, where the number of accumulated laser pulses per spot (N) was $\approx$60.

To enrich the surface treated by the laser beam with silanol groups serving as the centers for chemisorption of hydrophobic agents,[24] we exposed selected samples to UV−ozone treatment (Bioforce Laboratories) for 40 min.

The method of surface conductivity analysis described in our previous paper[10] was used to study the specific surface resistance of superhydrophobic coatings on glass substrates and the evolution of this resistivity on long-term contact with saturated water vapor and bulk water.

The measurement setup consists of two principal parts: a TOmM-1 teraohmmeter (NPP Norma) operating at a voltage of 1000 V and an IK-01m measurement chamber. As we have shown,[10] the specific surface resistance of dielectric materials such as silicon rubber or glass is very sensitive to the presence of water molecules adsorbed on the insulator surface and/or embedded in the surface dielectric layers.

To characterize coating wettability, we measured the contact and rolling angles using digital video image processing of sessile droplets.[25] The measured initial contact angles correspond to advancing contact angles, as follows from the behavior of the contact diameter. To characterize the wetting of different coatings, initial contact angles for 15 μL droplets were measured at 10 different surface locations for each sample. To measure the rolling angle, 15 μL droplets were deposited on the surface. After the initial droplet shape had been equilibrated, manipulation with an angular positioner allowed us to change the sample surface tilt in a controllable manner and detect the rolling angle by averaging over 10 different droplets on the same substrate.

We studied the stability of the superhydrophobic state of the coating both on long-term contact with water at a saturated vapor pressure and under abrasive wear in an oscillating sand abrasion test. The chemical stability of the coating on long-term contact with water was studied by monitoring the evolution of the water contact angle, the base diameter of the water droplet, and the liquid surface tension as functions of time, as described in refs 24 and 26.

The robustness of the coating against abrasive wear was studied according to ASTM F735 in an oscillating sand abrasion test. The contact and rolling angles of a test sample with coating were first measured and recorded. The sample was then mounted on the bottom of a tray and covered with a 12.5 mm thick layer of quartz silica with particle diameters from 500 to 800 μm. The tray was affixed to a motorized platform (Vibramax 100, Heidolph) that reciprocates in a back-and-forth motion over a distance of 3 mm at a speed of 1000 strokes/min. Inertia causes the entire mass of the abrasive medium to shift significantly within the tray, resulting in abrasion of the specimen. After exposure to abrasion for time t, the results are measured as the change in contact and rolling angles. To take the measurements, the sample was taken from the tray, treated in an ultrasonic bath in distilled water for 3 min, dried with ash-free filter paper, and air-dried for 30 min.

The surface morphology was studied using a Supra 40 VP field emission scanning electron microscope (Carl Zeiss) equipped with an INCA PentaFETx3 detector (Oxford Instruments) for energy-dispersive X-ray spectroscopy (EDS). The very low conductivity of glasses results in the accumulation of electrons in the immediate vicinity of the beam impact, raising the local potential. Such high surface potentials can severely degrade scanning electron microscopy (SEM) images. Thus, observing insulating samples such as glasses via SEM with an incident beam energy of 5−20 keV is nearly impossible because of charging effects. To overcome charging problems, an amorphous conductive carbon layer approximately 20−30 nm thick was deposited on the surface of the glass sample. This thickness provided adequate conductivity, and charging effects were not observed. All X-ray spectra for microanalysis were generated at an acceleration voltage of 10 or 20 kV.

RESULTS AND DISCUSSION

Four types of samples differing from each other in their laser treatment parameters (see Table 1) were fabricated, followed by adsorption of a hydrophobic agent, as described above in Materials and Methods. The corresponding initial advancing angles, as well as the rolling angles for all samples, are listed in the right-hand columns of Table 1. As follows from the experimental data, samples 1, 3, and 4 show the water droplet rolling from the inclined sample surface and contact angles

Table 1. Laser Treatment and Wetting Parameters for Different Glass Samples

sample	overlap step l (μm)	linear scanning rate v (mm/s)	repetition rate f (kHz)	contact angle (deg)	rolling angle (deg)
1	18	3	500	156.8 ± 2.3	26.7 ± 9.8
2	6	6	500	120.9 ± 2.9[a]	–
3	6	6	50	161.9 ± 2.6	8.5 ± 2.6
4	18	3	50	166.6 ± 5.6	12.2 ± 7.1

[a]The receding angle for the sample 2 was 81.1 ± 3.2°.

dx.doi.org/10.1021/am4051603 | ACS Appl. Mater. Interfaces 2014, 6, 2080−2085

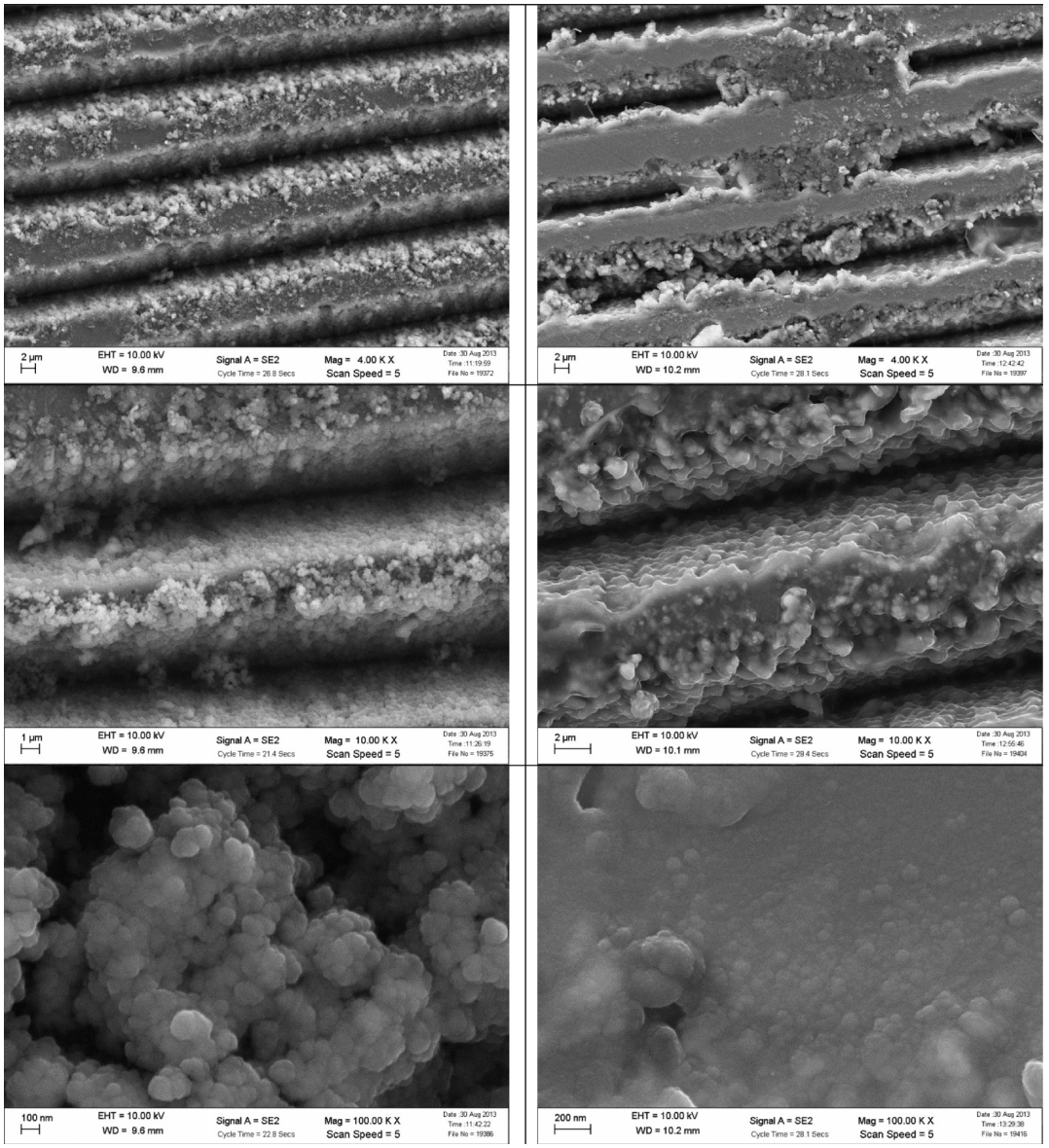

Figure 1. SEM images of glass sample 3′. The left column shows the morphology of surface after laser treatment, and the right column shows the same sample after the oscillating abrasion test.

exceeding 150°. Sample 3 showed the best uniformity of the contact and rolling angles and the smallest rolling angle. Thus, one may expect the best self-cleaning ability of such coating and its improved electro-insulating performance under exploitation conditions. Therefore, we used the laser treatment parameters characteristic of sample 3 as the base parameters for further studies. The morphology of sample 3 with multimodal surface relief is illustrated in Figure 1.

The analysis of the long-term stability of the superhydrophobic state indicated rather weak binding of the hydrophobic agent to the laser-treated glass surface. This analysis was based on monitoring the time evolution of the water contact angle, liquid surface tension, and base diameter of a water droplet atop a sample exposed to an atmosphere with 100% humidity inside the experimental chamber. The evolution of the water droplet contact angle and surface tension is shown in Figure 2 for sample 3 (lines 1 and 1′, respectively). The rapid deterioration of the contact angle, which is accompanied by a decrease in surface tension, indicates the process of essential desorption of fluorooxysilane molecules from the glass surface and their transfer from the solid−water interface to the water−air interface.

The main mechanism anchoring the molecules of the hydrophobic agent to the glass surface is chemisorption on the surface silanol groups.[24] Molecules that are physically deposited on the surface by van der Waals forces may be easily removed from the surface on contact with water. Thus, it may be inferred from our data that high-energy laser beam treatment of a glass surface results in cross-linking of the native silanol groups with the formation of siloxane bonds and therefore in a decreasing number of active sites that are available for chemical binding of molecules of the hydrophobic agent to the glass surface.

To enrich the glass surface with chemisorption centers, we exposed the laser-modified samples to UV−ozone treatment. After this two-stage modification, the glass surface showed complete wetting by water. Subsequent drying in an oven and immersion in a decane solution of the hydrophobic agent as

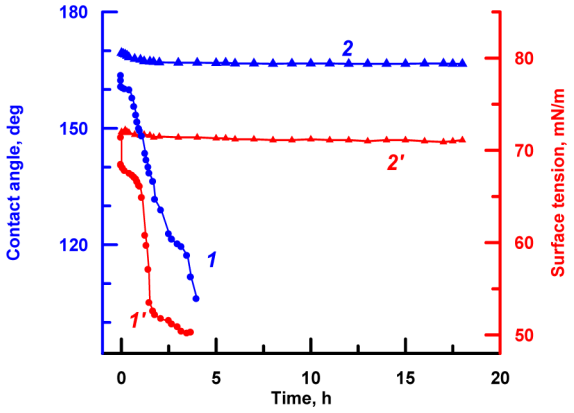

Figure 2. Time evolution of the contact angle (1 and 2) and surface tension (1′ and 2′) of the sessile water droplet during long-time contact with the surface of laser-textured glass hydrophobized without (1 and 1′) and with (2 and 2′) additional UV−ozone treatment before the hydrophobization.

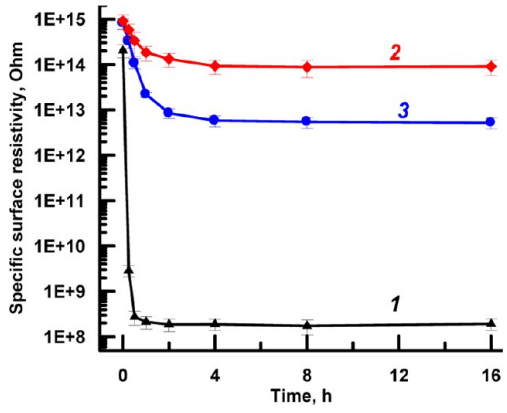

Figure 3. Dependence of the specific electrical surface resistance of untreated glass (1) and glass sample 3′ with textured superhydrophobic coating before (2) and after a 35 min abrasion test (3) on the time of sample exposure to saturated water vapor.

described above establish the superhydrophobic state of the glass surface. Sample 3′, which was subjected to UV−ozone treatment after laser treatment with the parameters listed in Table 1 for sample 3, had a contact angle that was larger than that of a similar sample hydrophobized without UV−ozone treatment. For this sample, the characteristic values of the contact angle were 165.7 ± 3.3°, and rolling angles were less than 10° (Table 2). Monitoring the contact angle and surface tension behavior for sample 3′ now indicates the long-term stability of the superhydrophobic state of a glass surface in contact with water (Figure 2).

Table 2. Variation of Surface Wettability of Samples Subjected to the Oscillating Sand Abrasion Test

	superhydrophobic sample 3′		hydrophobic sample
time of abrasive processing (min)	contact angle (deg)	rolling angle (deg)	contact angle (deg)
0	165.7 ± 3.3	8.7 ± 1.6	110.6 ± 3.9
5	113.4 ± 4.7	no rolling	85.4 ± 14.2
15	54.7 ± 4.7	no rolling	42.5 ± 8.3
35	45 ± 5.9	no rolling	0[a]

[a]After 30 min of exposure to air, the contact angle value increased to 21.3 ± 5.7°.

We studied the electro-insulating properties of a superhydrophobic coating on sample 3′, which was fabricated with the same laser treatment parameters used for sample 3 but was subjected to UV−ozone pretreatment before the adsorption of a hydrophobic agent. In Figure 3, the specific surface resistances for an untreated glass sample and glass with a superhydrophobic coating are shown as a function of exposure time of the samples to 100% humidity. It is worth noting that under operating conditions, electro-insulating materials are in contact with air characterized by a high relative humidity. That is why we studied the electro-insulating properties of the coating on sample 3′ after long-term contact with saturated water vapor. As we showed in our recent paper,[10] exposure of superhydrophobic and hydrophobic coatings to a humid atmosphere is accompanied by the formation of wetting/adsorption water films on the coatings causing a decrease in surface resistivity. The data presented in Figure 3 show that some deterioration of the insulating properties of the superhydrophobic coating on sample 3′ occurs during contact with humid air. However, after exposure for 4 h, the specific surface resistivity (ρ_s) reaches a plateau with a value on the order of hundreds of teraohms. By comparison, the surface resistivity of untreated glass decreases to fractions of a gigaohm, indicating the formation of thick surface water layers.

These data correlate well with the analysis performed in ref 10, where it was shown that the decrease in surface resistivity of electro-insulating materials in a humid atmosphere is associated with the conductivity of a thin water layer that is formed on the surface. The thickness and conductivity of such a layer are greater as the surface wettability improves and as the number of water soluble or hydrating surface contaminations increases. For the superhydrophobic surfaces. the formation of an adsorption discontinuous water layer is characteristic in contrast to multilayer wetting films on hydrophilic materials.

The surface resistivity of both an untreated glass sample and glass with a superhydrophobic coating was measured after the samples had been immersed in bulk water for 48 h, taken out, and dried with ash-free filter paper. The ρ_s values characteristic of untreated glass and glass with a superhydrophobic coating were 1.32×10^{14} and 7.16×10^{14} Ω, respectively, indicating that glass with a superhydrophobic coating has much better electro-insulating properties.

The block of data presented above shows the very attractive electro-insulating properties of glass substrates with superhydrophobic coatings. However, the key question about using these coatings in outdoor electroenergetics is the resistance of electro-insulating properties to the abrasive wear associated with blasting the surface of construction elements with solid dust particles. Various methods for estimating the mechanical stability of superhydrophobic coatings against abrasion load have been used in the literature (see, for example, refs 27−29). To evaluate the preservation of electro-insulating properties and the evolution of wettability, we subjected a glass sample with a superhydrophobic coating to the oscillating sand abrasion test and monitored the influence of time of the abrasive treatment on the surface morphology, contact angle, and surface resistivity. The evolution of wettability parameters versus time of the abrasion test is presented in Table 2. The same test was performed with a hydrophobic coating deposited on an untreated glass substrate for comparison. As follows from the experimental data, the initially hydrophobic sample loses its

dx.doi.org/10.1021/am4051603 | ACS Appl. Mater. Interfaces 2014, 6, 2080−2085

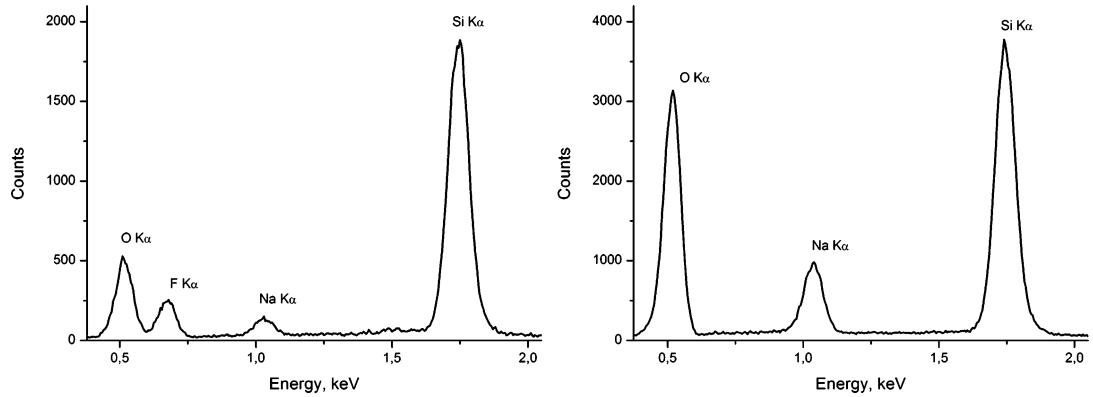

Figure 4. EDS spectra, characterizing the chemical composition within the grooves (left) and that on the top of ridges (right), taken from sample 3′ subjected to the 35 min oscillating sand abrasion test. The absence of a fluorine peak on the spectrum taken from the top of the ridge indicates the abrasive removal of the hydrophobic agent from corresponding patches on the surface.

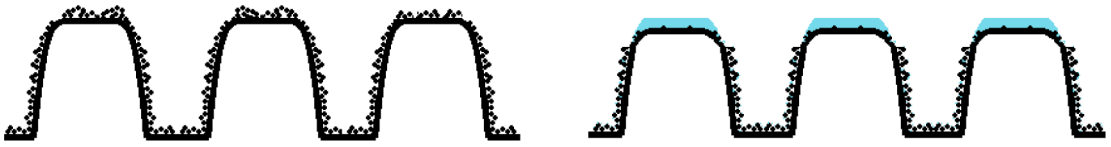

Figure 5. Schematic explanation of the enhanced conductivity of a laser-textured surface of glass after an abrasion test. Before the abrasion test (left), the surface conductivity is extremely low because of the absence of a conductive water layer atop the electro-insulating coating. After the abrasion test (right), the replacement of surface hydrophobic texture by the hydrophilic glass surface is accompanied by the formation of water films on hydrophilic patches (colored blue) in a humid atmosphere. The presence of electro-insulating bridges separating the conductive water layers favors the good electro-insulating performance of superhydrophobic coatings on glass even after the abrasion test.

hydrophobicity within the first 5 min of abrasive wear. After 15 min, numerous abrasion marks on the sample surface are detected visually. After 35 min, the sample shows significant abrasion delustering and complete wetting by water. The abrasion process is accompanied by local deformations of the surface and thus by an increase in surface energy. This phenomenon is known as thermo-mechanical activation of the surface. That is why just after abrasion treatment, the sample surface state is highly nonequilibrium with enhanced adsorption activity. Such adsorption activity on the surface of thermo-mechanically activated materials is driven by the tendency to reduce the total free (Gibbs) energy of the system by decreasing the surface energy. Thus, from the perspective of thermodynamics, the surface of abraded glass tends to be enhanced by airborne adsorbates that decrease its surface energy. As a result, the contact angle increases to 21.3 ± 5.7° after exposure to ambient air for 30 min. The superhydrophobic coating shows the longer durability of the hydrophobic state, although superhydrophobicity is lost after sand abrasion for <5 min. However, the essential part of the coating still contains patches that are wetted in the heterogeneous regime with preservation of the superhydrophobic state within the grooves. We analyzed the surface morphology and specific surface resistance of a superhydrophobic sample subjected to the oscillating sand abrasion test for 35 min. The morphology presented in the right-hand column of Figure 1 indicates two different processes. The first process leads to the detachment of nanoparticles fabricated on the surfaces during laser treatment from the tops of ridges. The second one is typical of glass grinding and polishing and is associated with the melting and smoothing of microridges. In both processes, hydrophobic surface patches are replaced by hydrophilic ones on the tops of ridges.

As a result, the formation of a patched surface with a multimodal superhydrophobic nature inside the grooves and hydrophilic smoothened patches without a hydrophobic agent on the tops leads to surface wettability with an effective contact angle defined by the Cassie equation for a chemically heterogeneous surface.[30] EDS analysis of the surface composition associated with the patches inside the grooves (Figure 4, left) and on the tops of ridges (Figure 4, right) proves the conclusions derived from the results of wettability measurements.

The peculiarities of surface texture with a ripple structure are the reason why abrasive wear causes the formation of only hydrophilic stripes with better conductivity but separated by hydrophobic grooves with strong electro-insulating properties. Therefore, the electro-insulating properties of the sample as a whole are preserved, at least under saturated vapor conditions. The surface resistivity of a superhydrophobic glass sample subjected to a 35 min oscillating sand abrasion test was measured after long-term contact with a humid atmosphere to check this idea. The results of these measurements for different exposure times (Figure 3) indicate that the electro-insulating performance of glass samples with a superhydrophobic coating is still considerably better than for untreated glass insulators, even after a very intensive abrasion load. As a consequence, the leakage currents over glass construction elements with superhydrophobic coatings remain a few orders of magnitude lower than those for untreated glass. The schematic presentation of a sample surface before and after the abrasion test in a damp atmosphere is given in Figure 5.

CONCLUSIONS

Femtosecond laser treatment of a glass surface was used in this study to fabricate a multimodal texture having regular surface ripples with a period of a few micrometers decorated by

dx.doi.org/10.1021/am4051603 | ACS Appl. Mater. Interfaces 2014, 6, 2080−2085

aggregates of nearly spherical nanoparticles. Adsorption of a hydrophobic agent, functional fluorosilane, on the fabricated texture results in a surface with superhydrophobic properties characterized by contact angles well above 160° and rolling angles of <10°. However, in the case of physical adsorption of the hydrophobic agent on the glass surface, the stability of the adsorbed layer in contact with aqueous media is low. It was shown that the additional step of UV−ozone surface pretreatment to enrich the surface with surface hydroxyl groups acting as centers for chemical adsorption increases the resistance of the adsorbed layer of the hydrophobic agent to long-term contact with water. The study of the surface resistance of fabricated coatings shows that glass-based materials with superhydrophobic coatings may be considered one of the best modern electro-insulating materials. The data of the oscillating sand abrasion test indicate that these coatings are not highly resistant to abrasive wear, and the superhydrophobic state of the surface as a whole was lost after an intensive abrasion load for a few minutes. At the same time, the main advantage of the fabricated coating is the significant durability of its electro-insulating properties. The longevity of high surface resistivity, even on long-term contact with a water vapor-saturated atmosphere, is directly related to the peculiarities of surface texture and ripple structure allowing preservation of the superhydrophobic state of the surface in the grooves.

AUTHOR INFORMATION

Corresponding Author

*E-mail: boinovich@mail.ru.

Notes

The authors declare no competing financial interest.

ACKNOWLEDGMENTS

This study was financially supported by the Programs for fundamental studies of Presidium of the Russian Academy of Sciences "Fundamental bases of technologies of nanostructures and nanomaterials", "Development of Methods of Synthesis of Chemical Compounds and Design of New Materials", and a grant for the support of leading scientific schools of the Russian Federation (Project NSh-6299.2012.3).

REFERENCES

(1) Li, J.; Zhao, Y.; Hu, J.; Shu, L.; Shi, X. *J. Adhes. Sci. Technol.* **2012**, *26*, 665−679.

(2) Pathak, D.; Satwani, M.; Patel, M.; Patel, C. The Development of Silicone Rubber Composite Insulators in Power System. *Proceedings of the International Conference on Control Automation, Communication and Energy Conservation INCACEC 2009*, Perundurai, India, June 4−6, 2009; Allied Publishers Ltd.: New Delhi, 2009; Vol. *II*, pp 919−923.

(3) Watanabe, T. *J. Ceram. Soc. Jpn.* **2009**, *117*, 1285−1292.

(4) Reinosa, J. J.; Romero, J. J.; Rubia, M. A.; Campo, A.; Fernandez, J. F. *Ceram. Interfaces* **2013**, *39*, 2489−2495.

(5) Mahadik, S. A.; Fernando, P. D.; Hegade, N. D.; Wagh, P. B.; Gupta, S. C. *J. Colloid Interface Sci.* **2013**, *405*, 262−268.

(6) Aytug, T.; Simpson, J. T.; Lupini, A. R.; Trejo, R. M.; Jellison, G. E.; Ivanov, I. N.; Pennycook, S. J.; Hillesheim, D. A.; Winter, K. O.; Christen, D. K.; Hunter, S. R.; Haynes, J. A. *Nanotechnology* **2013**, *24*, 315602.

(7) Wang, S. D.; Shu, Y. Y. *J. Coat. Technol. Res.* **2013**, *10*, 527−535.

(8) Infante, D.; Koch, K. W.; Mazumder, P.; Tian, L. L.; Carrilero, A.; Tulli, D.; Baker, D.; Pruneri, V. *Nano Res.* **2013**, *6*, 429−440.

(9) Oliveira, N. M.; Reis, R. L.; Mano, J. F. *ACS Appl. Mater. Interfaces* **2013**, *5*, 4202−4208.

(10) Pashinin, A. S.; Emel'yanenko, A. M.; Boinovich, L. B. *Prot. Met. Phys. Chem. Surf.* **2010**, *46*, 734−739.

(11) Dopierala, K.; Maciejewski, H.; Karasiewicz, J.; Prochaska, K. *Appl. Surf. Sci.* **2013**, *283*, 453−459.

(12) Athauda, T. J.; Williams, W.; Roberts, K. P.; Ozer, R. R. *J. Mater. Sci.* **2013**, *48*, 6115−6120.

(13) Cho, Y. S.; Moon, J. W.; Lim, D. C.; Kim, Y. D. *Korean J. Chem. Eng.* **2013**, *30*, 1142−1152.

(14) Li, X. Y.; He, J. H. *ACS Appl. Mater. Interfaces* **2012**, *4*, 2204−2211.

(15) Goswami, D.; Medda, S. K.; De, G. *ACS Appl. Mater. Interfaces* **2011**, *3*, 3440−3447.

(16) Irzh, A.; Ghindes, L.; Gedanken, A. *ACS Appl. Mater. Interfaces* **2011**, *3*, 4566−4572.

(17) Boinovich, L. B. *Herald Russ. Acad. Sci.* **2013**, *83*, 8−16.

(18) Vorobyev, A. Y.; Guo, C. *Laser Photonics Rev.* **2013**, *7*, 385−407.

(19) Stratakis, E. *Sci. Adv. Mater.* **2012**, *4*, 407−431.

(20) Golosov, E. V.; Emel'yanov, V. I.; Ionin, A. A.; Kolobov, Yu. R.; Kudryashov, S. I.; Ligachev, A. E.; Novoselov, Yu. N.; Seleznev, L. V.; Sinitsyn, D. V. *JETP Lett.* **2009**, *90*, 107−110.

(21) Ionin, A. A.; Kudryashov, S. I.; Seleznev, L. V.; Sinitsyn, D. V.; Emel'yanov, V. I. *JETP Lett.* **2013**, *97*, 121−125.

(22) Bonse, J.; Krüger, J. *J. Appl. Phys.* **2010**, *108*, 034903.

(23) Usoskin, A.; Freyhardt, H. C.; Krebs, H. U. *Appl. Phys. A: Mater. Sci. Process.* **1999**, *69*, S823−S826.

(24) Boinovich, L.; Emelyanenko, A. *Adv. Colloid Interface Sci.* **2012**, *179*, 133−141.

(25) Emel'yanenko, A. M.; Boinovich, L. B. *Inorg. Mater.* **2011**, *47*, 1667−1675.

(26) Boinovich, L. B.; Emelyanenko, A. M.; Pashinin, A. S. *ACS Appl. Mater. Interfaces* **2010**, *2*, 1754−1758.

(27) Deng, X.; Mammen, L.; Zhao, Y.; Lellig, P.; Müllen, K.; Li, C.; Butt, H.-J.; Vollmer, D. *Adv. Mater.* **2011**, *23*, 2962−2965.

(28) Gemici, Z.; Shimomura, H.; Cohen, R. E.; Rubner, M. F. *Langmuir* **2008**, *24*, 2168−2177.

(29) Xue, C.; Ma, J. *J. Mater. Chem. A* **2013**, *1*, 4146−4161.

(30) Cassie, A. B. D. *Discuss. Faraday Soc.* **1948**, *3*, 11−16.